Level structure of odd-mass Pr isotopes: Decay of 3.0-min ^{145}Ce to levels of ^{145}Pr

E. M. Baum,* J. D. Robertson,† P. F. Mantica, Jr., S. H. Faller,‡
C. A. Stone,§ and W. B. Walters
Department of Chemistry, University of Maryland, College Park, Maryland 20742

R. A. Meyer
Nuclear Chemistry Division, Lawrence Livermore National Laboratory, Livermore, California 94550

D. F. Kusnezov**
Department of Physics, Princeton University, Princeton, New Jersey 08540
(Received 11 July 1988)

The structure of ^{145}Pr has been investigated by measuring the gamma-ray singles, gamma-ray coincidence, and gamma-ray angular correlation spectra, along with conversion-electron singles spectra for the decay of 3.0-min ^{145}Ce to levels of ^{145}Pr. A level scheme is proposed that includes a number of new levels as well as new spin and parity assignments for several levels. The conversion-coefficient measurements establish the presence of a low-energy $\frac{3}{2}^-$ level at 787 keV whose strong population in beta decay confirms negative parity for the ground state of ^{145}Ce. Interacting boson-fermion model calculations for ^{143}Pr and ^{145}Pr are found to be in reasonable agreement with the observed low-energy positive-parity levels, while the presence of the low-energy $\frac{3}{2}^-$ level suggests the coexistence of more deformed configurations.

I. INTRODUCTION

The structure of the odd-Z Pr nuclides play a crucial role in the development of a theoretical description of the structure of the nuclides that lie between ^{132}Sn and ^{154}Gd. The lighter odd-Z nuclides $_{51}$Sb, $_{53}$I, $_{55}$Cs, and $_{57}$La can be readily considered as having 1, 3, 5, and 7 protons, respectively, beyond the closed proton shell at $Z=50$. The heavier odd-Z nuclides $_{61}$Pm and $_{63}$Eu can be considered as having one and three holes, respectively, in the closed proton subshell at $Z=64$.[1,2] Studies of neutron-proton interactions by Casten, Frank, and von Brentano have shown[3] that these nuclides approach deformation along a curve that is separate from those that lie beyond ^{154}Gd.

The structures of the odd-Z, closed-shell $N=82$ nuclides have been investigated in detail through in-beam reaction studies and radioactive decay, as well as by both proton stripping and pickup reactions.[4–6] Their structures are shown in Fig. 1. These data have permitted a detailed set of proton occupancy values to be determined for the set of five single-particle orbitals whose positions vary only slightly between $Z=50$ and 64. The changes of position of the quasiparticle levels shown in Fig. 1 can be attributed to the filling of a nearly constant set of single-particle levels and the upward motion of the Fermi level.[7] These observed level structures have been described in detail by weak-coupling pairing plus quadrupole models.[8] Considerable support for these occupancy values has been found in the multiplet structures of the odd-odd $N=83$ isotones,[9] where the splitting of the proton-neutron multiplets involving the $g_{7/2}$ and $d_{5/2}$ proton orbital and the single $f_{7/2}$ neutron is consistent with the occupancy values derived from the spectroscopic factors.

The effect of the addition of one pair of $f_{7/2}$ neutrons is shown in Fig. 2 where the structures of the odd-Z $N=84$ nuclides are shown. The proton occupancy values are found to change more slowly than in the $N=82$ isotones, particularly in ^{143}Pr, where the $g_{7/2}$ and $d_{5/2}$ levels are inverted. The extra pair of neutrons permits the neutron-proton interaction to enhance the longer-range quadrupole interactions relative to the short-range pairing interaction. The presence of one pair of neutrons reduces the occupancy of the $g_{7/2}$ level and increases the occupancy of the other proton orbitals and returns the $g_{7/2}$ orbital to a position closest to the Fermi level, and hence to the ground state. Spectroscopic factors are shown in Figs. 1 and 2 for the Pm nuclides for (^{3}He,d) reactions which reveal the dramatic changes induced for all five single-particle levels.[10] The structure of ^{141}La is also affected by the slower change of occupancies. In ^{139}La where the $N=82$ shell is closed, the $g_{7/2}$ proton orbital is sufficiently occupied so that three holes are not present to form a second low-energy $\frac{5}{2}^+$ state with a $(g_{7/2})^3_{5/2}$ configuration.[11] These cluster states are quite apparent in both ^{135}I and ^{137}Cs which have three particles and three holes, respectively, in the $g_{7/2}$ orbital.[12] In the $N=84$ isotones, the extra $\frac{5}{2}$ level is clearly present[13] in ^{137}I and ^{139}Cs as expected, and is also present in ^{141}La owing to the occupancy reduction induced by the pair of $f_{7/2}$ neutrons. Lee *et al.*[14] measured the cross sections for the (d,^{3}He) reactions on Sm nuclides that populate the levels of the odd-mass Pm nuclides from mass 147 through mass 153. From these data, they determined the changes of occupancy in the Pm nuclides with increasing numbers of neutrons, which revealed a significant shift of protons from the $g_{7/2}$ orbitals to the $h_{11/2}$ orbitals.

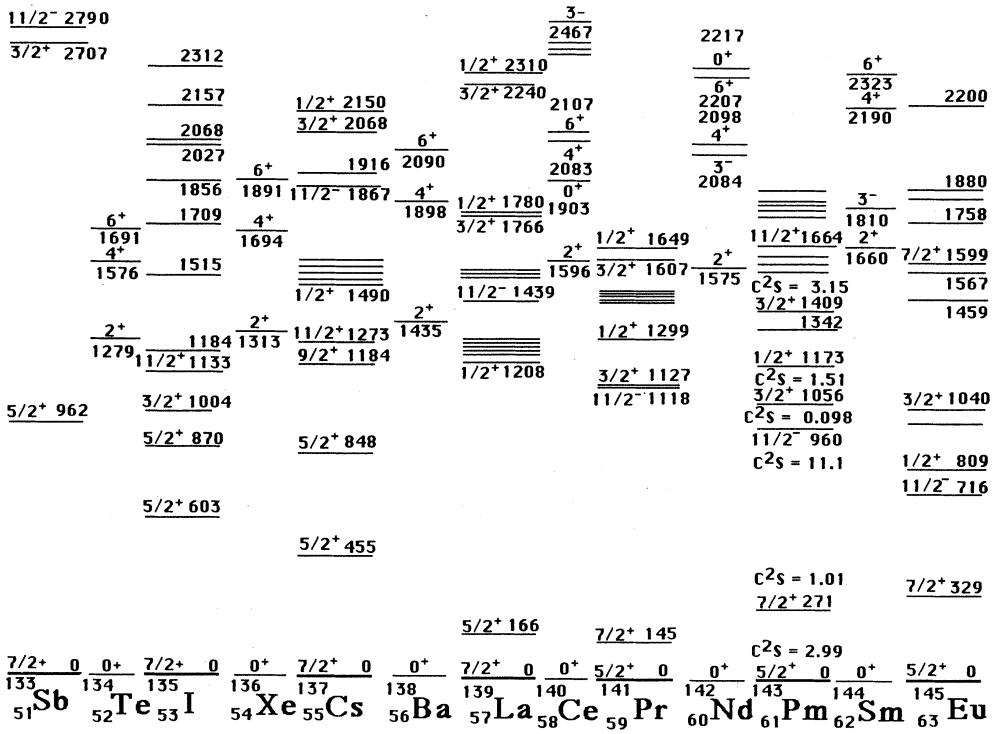

FIG. 1. Positions of the low-energy levels of the $N=82$ isotones. The spectroscopic factors shown for the ^{142}Nd(^{3}He,d)^{143}Pm reaction are taken from Ref. 7.

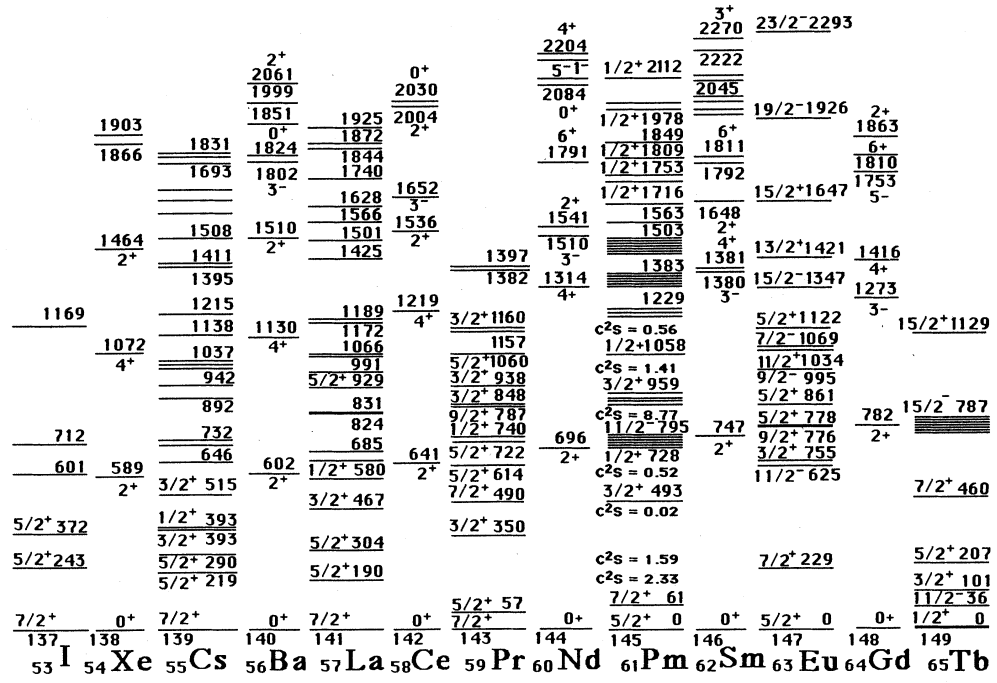

FIG. 2. Positions of the low-energy levels of the $N=84$ isotones. The spectroscopic factors shown for the ^{144}Nd(^{3}He,d)^{145}Pm reaction are taken from Ref. 7.

Because of these occupancy shifts, an increasingly complex description is required for these odd-Z nuclides as neutrons are added beyond $N=82$, particularly to account for the onset of strong deformation that occurs at $N=90$. For the Eu and Sm isotopes, ground-state moments and radii[15,16] support the presence of a sharp transition with only limited deformation present through $N=88$. The degree to which this transition is sharply defined is not so well established in the lighter Z nuclides. The measured g factors for the first 2^+ levels of the even even Nd, Ce, and Ba nuclides suggest a more gradual change, which can be understood with effective boson numbers determined from the slow disappearance of the $Z=64$ subshell closure.[17–19] Even more complex configurations have been indicated by several other studies which support the presence of reflection asymmetric structures[20–22] in the region near ^{145}Ba. The positive-parity levels of the odd-Z Eu and Pm nuclides[1] have been reasonably well described by the interacting boson-fermion model (IBFM), but the negative-parity levels, particularly the low-spin levels in Pm, are not well fit in either the IBFM calculations[2] or in intermediate coupling calculations.[23]

Previous studies of the structure of ^{145}Pr have led to the establishment of levels at 63, 347, 351, 555, 787, 846, and 1211 keV. In three studies of the decay of 3.0-min ^{145}Ce to levels of ^{145}Pr, additional levels have been proposed[24–27] at 189, 783, 859, 1245, 1456, and 1465 keV. In three reports of the results of the population of ^{145}Pr levels in $(d,{}^3\mathrm{He})$ reactions[28–30] on ^{146}Nd, levels near 60, 190, 540, 750, and 1080 keV were consistently observed, with additional levels at 337, 745, 810, 1244, 1333, and 1490 keV possible. In contrast, extensive in-beam, transfer, and decay studies have led to well-established, detailed level schemes[31,32] for the heavier $N=86$ isotones, ^{147}Pm and ^{149}Eu. In previous papers, we have reported new results[33,34] for the structures of the lighter $N=86$ isotones ^{141}Cs and ^{143}La. In this paper, new results for the structure of ^{145}Pr are reported, and in a companion paper, new results are presented for the decay of ^{143}Ce to levels of the $N=84$ nuclide ^{143}Pr.[35]

II. EXPERIMENTAL PROCEDURES

This study of the decay of ^{145}Ce to levels of ^{145}Pr was performed at the TRISTAN on-line mass separator facility at the High Flux Beam Reactor (HFBR) located at Brookhaven National Laboratory. The description of the facility and the surface ionization ion source used to produce the desired activity has been described in previous publications.[36–38]

The ion beam was deposited on a continuous mylar tape at the parent port of the moving tape collector for three minutes. The primary fission product extracted at mass 145 is ^{145}Cs. After the 3.0-min deposition time, the tape was moved to a point halfway between the parent and daughter ports and allowed to decay for 3 min. This allowed time for all of the 0.58-s ^{145}Cs, 4.0-s ^{145}Ba, and 25-s ^{145}La to decay to ^{145}Ce. The tape was then moved to the daughter port, where it was counted for 3 min while new sources were depositing and growing.

Experimental angular-correlation data were collected using a four detector coincidence array located around the daughter port of the moving tape collector. The detector arrangement consisted of four Ge(Li) detectors located 7.5 cm from the source. The detectors were arranged at 90° to each adjacent detector, giving four 90° pairs and two 180° pairs of detectors for angular-correlation studies. The angular-correlation system was calibrated using the $2^+(M1/E2)2^+(E2)0^+$ and the $3^-(E1)2^+(E2)0^+$ transitions in ^{142}Ce in a separate experiment and in similar transitions in ^{144}Ce which was present as a result of delayed neutron emission following the decay of ^{145}Cs. Coincidences were recorded on magnetic tape as three parameter events: E_{c1}, E_{c2}, and the time interval between the two gamma rays. The duration of the collection of these data was 131 h, with an average activity at the daughter port of 3500 cps on each detector. Using a similar deposit and decay cycle, conversion-electron spectra were measured at the 0° beam line using a Si(Li) detector system that has also been described previously.[7]

III. EXPERIMENTAL RESULTS

Gamma rays assigned to the decay of 3.0-min ^{145}Ce are tabulated in Table I and the conversion-electron intensities are tabulated in Table II. The gamma rays observed in a number of the coincidence gates are tabulated in Table III. Intensities for the low-energy transitions were determined using a small planar Ge detector whose efficiency curve was calibrated with a National Institute of Standards and Technology (NIST) standard reference source. The resulting level scheme is shown in Fig. 3. The comparison of the measured conversion coefficients with calculated conversion coefficients[39] establish the $E1$ character of the intense 724-keV transition as well as the $M1/E2$ character of the 63-, 285-, and 424-keV transitions. In turn, these data establish negative parity for the levels at 787 and 1211 keV. As these levels are fed in beta decay with logft values near 5, negative parity is also established for the ground state of ^{145}Ce and the spin of ^{145}Ce is limited to $\frac{3}{2}$ or $\frac{5}{2}$. Extensive coincidence data, some of which are shown in Fig. 4, support previously proposed levels at 189, 859, and 1111 keV and indicate new levels at 540, 696, 766, 806, 836, 846, 1047, 1318, 1331, 1560, and 1609 keV.

The most intense transition with multiple placements is the 351-keV transition, whose coincidence gate is shown in Fig. 4. The gate on the 724-keV gamma ray shows that only the 424-keV gamma ray populates the 787-keV level and that the 724-keV gamma ray is in full coincidence with the 63-keV transition. The gate on the 435-keV transition shows the 424-keV peak as well as an intense peak at 351 keV and lower-intensity peaks at 288 and 63 keV. This gate establishes the level at 351 keV and the ratio of the intensities of the 288- and 351-keV gamma rays that depopulate this level. The gate on the 351-keV peak shows all of the peaks listed in Table II including peaks at 126, 189, and 512 keV. The position of the 189-keV level is established by the gates on the 657-, 671-, 760-, and 858+860-keV peaks. The intensity of the

351-keV peak in the 126- and 189-keV gates is much larger than the others and requires direct population of the 189-keV level. Thus, there must be a second 351-keV transition that populates the 189-keV level from the level at 540 keV. The 670-keV gate shows low-intensity peaks at 540 and 477 keV and intense peaks at 126, 189, and 351 keV. The presence of the 126-keV peak assures that there is a cascade through the 189-keV level. However, the 189/126 intensity ratio in this gate is 1.5 times larger than the ratio in the 598-keV gate where the two peaks are of equal intensity. This disparity in ratios establishes the presence of a second 189-keV transition in this nuclide, one that populates the 351-keV level from the 540-keV level. No energy variation for the position of the 351-keV peak has been identified in any of the various gates, however.

TABLE I. Energies, intensities, and placements of gamma rays identified in the decay of ^{145}Ce to levels of ^{145}Pr.

Energy (keV)[a]	Relative intensity[a]	From	To	Energy (keV)[a]	Relative intensity[a]	From	To
62.54(2)	22.6(4)	63	0	554.83(3)	0.64(1)	555	0
125.3(1)		unplaced		597.9(1)	0.66(5)	787	189
126.07(2)	0.83(2)	189	63	634.54(6)	0.62(2)	696	63
158.5(3)	0.05(1)	347	189	645.6(1)	0.06(1)	unplaced	
188.85(1)	1.08(3)[b]	189	0	655.95(7)[c]	1.6(1)[b]	1211	555
189.2(3)	0.35(1)[b]	540	351	657.2(1)[c]	0.4(1)[b]	846	189
193.01(7)	0.19(2)	540	347	670.6(1)	0.8(1)[b]	1211	540
198.2(1)	0.38(2)	unplaced		670.6(1)	0.08(4)[b]	859	189
204.07(7)	0.06(2)	555	351	695.93(6)	0.17(1)	1047	351
207.61(1)	1.84(4)	555	347	701.4(2)	0.02(1)	1560	859
211.46(3)	0.080(3)	766	555	714.3(5)	0.04(2)	1560	846
232.08(1)	3.45(6)	787	555	724.33(3)	100	787	63
246.88(3)	0.24(1)	787	540	743.76(4)	0.24(1)	806	63
249.8(1)	0.09(1)	unplaced		759.74(5)	0.57(2)	1111	351
284.53(1)	13.8(2)	347	63	762.7(2)[c]	0.04(2)[b]	1609	846
288.4(1)	0.21(2)	351	63	763.24(6)	0.14(5)[b]	1111	347
304.66(7)	0.16(1)	859	555	773.19(6)[c]	0.31(5)[b]	836	63
319.4(1)	0.05(1)	859	540	773.24(6)[c]	0.10(2)[b]	1609	836
347.17(1)	1.31(2)	347	0	783.09(3)	3.98(6)	846	63
349		696	347	801.7(2)	0.05(1)	1609	806
350.9	4.30(5)[b]	351	0	831.4(1)	0.037(5)	unplaced	
350.9	1.54(2)[b]	540	189	835.0(1)	0.04(1)	836	01
350.9	1.52(2)[b]	1211	859	845.88(5)	0.51(1)	846	0
364.6(1)	0.06(1)	1211	846	858.11(6)[c]	0.3(1)[b]	1047	189
365.8(5)	0.05(3)	555	189	859.61(6)	2.8(1)[b]	1211	351
403.1(1)	0.037(5)	unplaced		863.31(5)	0.40(2)[b]	1211	347
423.60(3)	6.5(1)	1211	787	863.6(1)	0.02(1)[b]	1560	696
430.5(3)	0.05(1)	unplaced		872.1(1)	0.026(3)	unplaced	
435.99(4)	2.05(4)	787	351	885.5(1)	0.15(1)	949	63
439.71(4)	11.4(2)	787	347	911.91(8)	0.26(1)	1609	696
444.04(7)		1211	766	921.44(6)	0.25(1)	1111	189
447.18(7)	0.13(1)	unplaced		948.6(1)	0.08(1)	949	0
472.8(1)	0.04(1)	1318	846	953.6(2)	0.04(1)	unplaced	
477.2(1)	0.09(1)	540	63	968.92(7)	0.090(4)	unplaced	
482.5(1)	0.10(1)	1318	836	979.17(6)	0.15(1)	1331	351
492.21(3)	2.5(1)	555	63	1021.2(2)	0.06(2)	1211	189
498.97(3)	0.60(1)	846	347	1047.07(6)	0.16(1)	1047	0
507.3(2)[c]	0.15(3)[b]	1047	540	1110.68(4)	4.19(7)	1111	0
507.4(2)[c]	0.08(3)[b]	696	189	1148.03(4)	15.5(2)	1211	63
512.21(7)[c]	1.4(3)[b]	859	347	1210.63(4)	1.60(1)	1211	0
512.61(8)[c]	0.3(1)[b]	1211	696	1371.1(1)	0.12(1)	1560	189
517.9(6)	1.2(4)	unplaced		1497.7(1)	0.08(1)	1560	63
524.8(4)	0.02(1)	1312	806	1545.7(2)	0.03(1)	1609	63
540.36(5)	0.67(2)	540	0	1560.58(8)	0.06(3)	1560	0
				1607.1(2)	0.02(1)	1609	0

[a]The uncertainties in the last digit(s) of the energy and intensity values are shown in parentheses.
[b]The intensity value was derived using both singles and coincidence data.
[c]The energy value was derived using both singles and coincidence data.

TABLE II. Experimental internal conversion coefficients ($\times 10^2$).

Transition	Conversion coefficient	Theoretical[a] $M1$	$E2$	$E1$	Deduced multipolarity
284 K	6.4±1.9	6.28	4.68	1.27	$M1/E2$
351 K	2.7±0.7	3.64	2.52	0.75	$M1/E2$
724 K	0.17±0.04	0.60	0.38	0.15	$E1$

[a]The theoretical conversion coefficients are taken from Ref. 39.

TABLE III. Selected gamma-gamma coincidence results from the decay of ^{145}Ce to levels of ^{145}Pr.

Gated gamma ray (keV)	Gamma rays observed in coincidence (keV)							
63	126	193	208	232	247	285	288	351
	424	440	492	499	512	635	656	671
	724	744	763	773	783	860	863	886
	912	1148	1371	1498				
126	63	159	208	232	247	351	366	492
	507	598	656	671	860	921	1021	1371
159	63	126	189	208	232	440		
189	208	232	247	285	351	366	440	598
	656	671	860	921	1021			
204	63	232	285	351	424	444	512	656
208	63	211	232	285	289	305	347	351
	424	656						
211	189	208	285	351	444	492		
232	63	204	208	285	347	351	424	440
	492	555						
247	63	126	189	351	424	477	540	
285	63	193	208	232	305	351	424	440
	499	512	656	671	763	863		
288	63	436	440	860				
305	63	126	189	208	285	351	492	656
319	126	189	232	351				
347	63	208	232	284	351	424	436	440
	512	656	860	863				
351	63	126	189	204	208	211	232	247
	285	305	319	347	351	436	440	444
	492	507	512	671	696	724	860	979
365	63	284	351	499	783			
424	63	189	208	232	247	285	347	351
	436	440	492	724				
436/440	285	288	351	424				
444	211	285	351					
473	63	285	351	499	783			
492	63	211	232	305	351	424	656	
499	63	285	347	351	365	473	763	
507	63	126	189	351	477	912		
512	63	285	347	351	424	440	635	701
540	247	351	397	671				
635	63	512	863	912				

TABLE III. (*Continued*).

Gated gamma ray (keV)	Gamma rays observed in coincidence (keV)							
656	63	126	189	208	285	347	351	492
	555							
671	126	189	193	285	288	351	477	540
724	63	424						
744	525	802						
760	63	126	189	285	288	351		
763	63	285	347	351	499	783		
773	63	483	773					
783	63	365	473	714	763			
802	744							
858/860	63	126	189	285	288	351		
863	63	285	347					

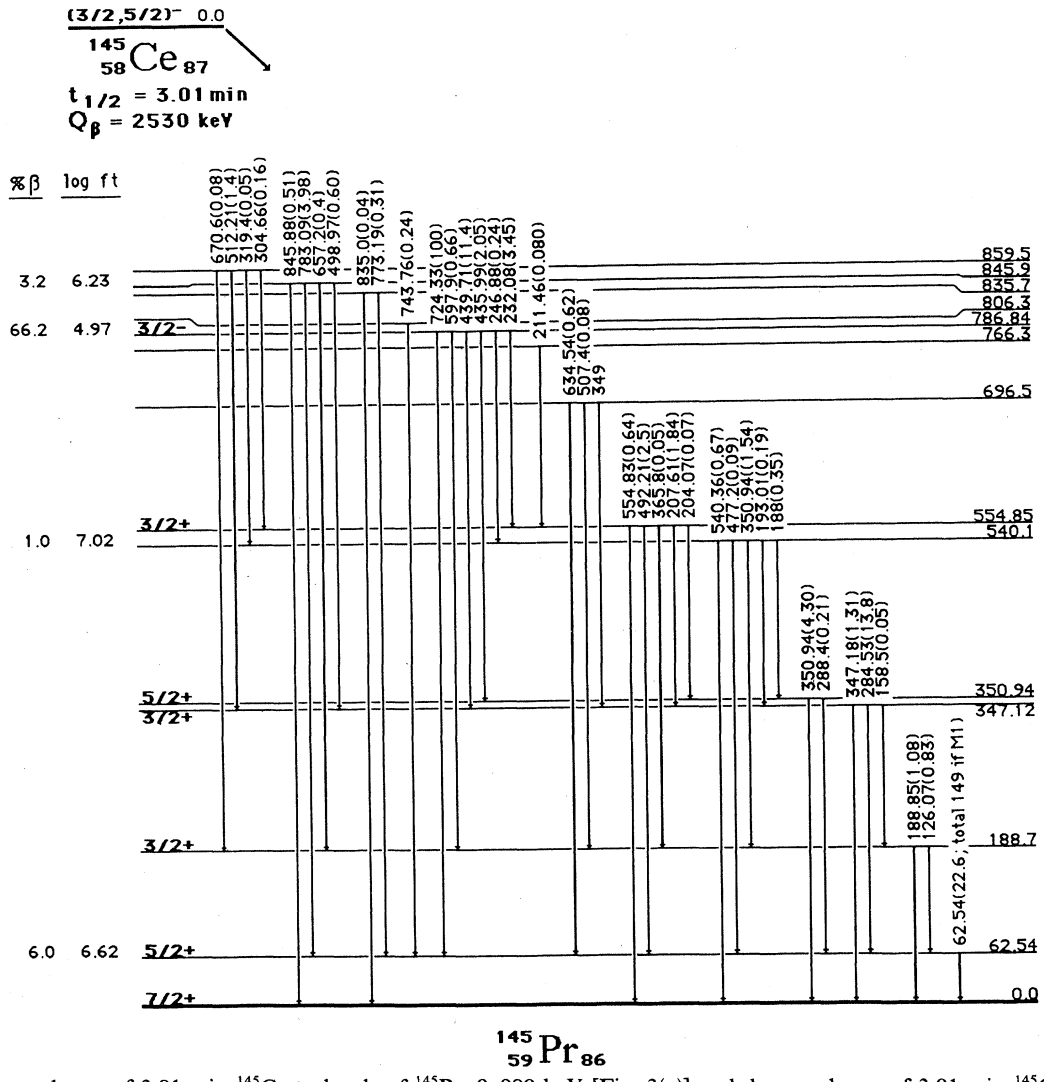

FIG. 3. Decay scheme of 3.01-min ^{145}Ce to levels of ^{145}Pr, 0–900 keV [Fig. 3(a)] and decay scheme of 3.01-min ^{145}Ce to levels of ^{145}Pr, 900–1610 keV [Fig. 3(b)].

The third 351-keV transition is suggested by the presence in the 351-keV gate of a peak at 351 keV. The 635-keV gate shows two intense peaks at 63 and 512 keV and two very low-intensity peaks at 863 and 912 keV. The two intense peaks establish a cascade from the intensely populated 1211-keV level to the 63-keV level. The two low-intensity peaks suggest that the intermediate level is at 635 keV. The gate on the 512-keV peak shows low-intensity peaks at 635 keV (268 counts) and 63 keV consistent with the cascade from the 1210-keV level. Much more intense peaks of approximately equal size (2500 counts) are found at 285 and 351 keV implying a second cascade from the 1148-keV level that requires either a third 351-keV transition or a second 285-keV transition. The presence of the 347-keV peak in the correct ratio to the 285-keV peak gives assurance that this cascade populates the 347-keV level. Peaks in the 351-keV gate at 305, 319, 507, and 671 keV and a very low-intensity peak in the 512-keV gate at 701 keV all support the placements as shown. A slight distinction between the positions of the 512-keV peaks is observed in the various coincidence spectra.

The stronger member of the doublet at 671 keV clearly populates the 540-keV level and the gate on the 671-keV peak shows strong peaks at 63, 126, 189, and 351 keV, while the gate on the 540-keV ground-state transition clearly shows the 671-keV peak. But, the intensity of the 351-keV transition is too large relative to the intensity of the observed strength of the sum of the 126- and 189-keV transitions. This excess suggests that the extra intensity arises from the presence of a 671-keV transition that depopulates the level at 859 keV, which is fed almost en-

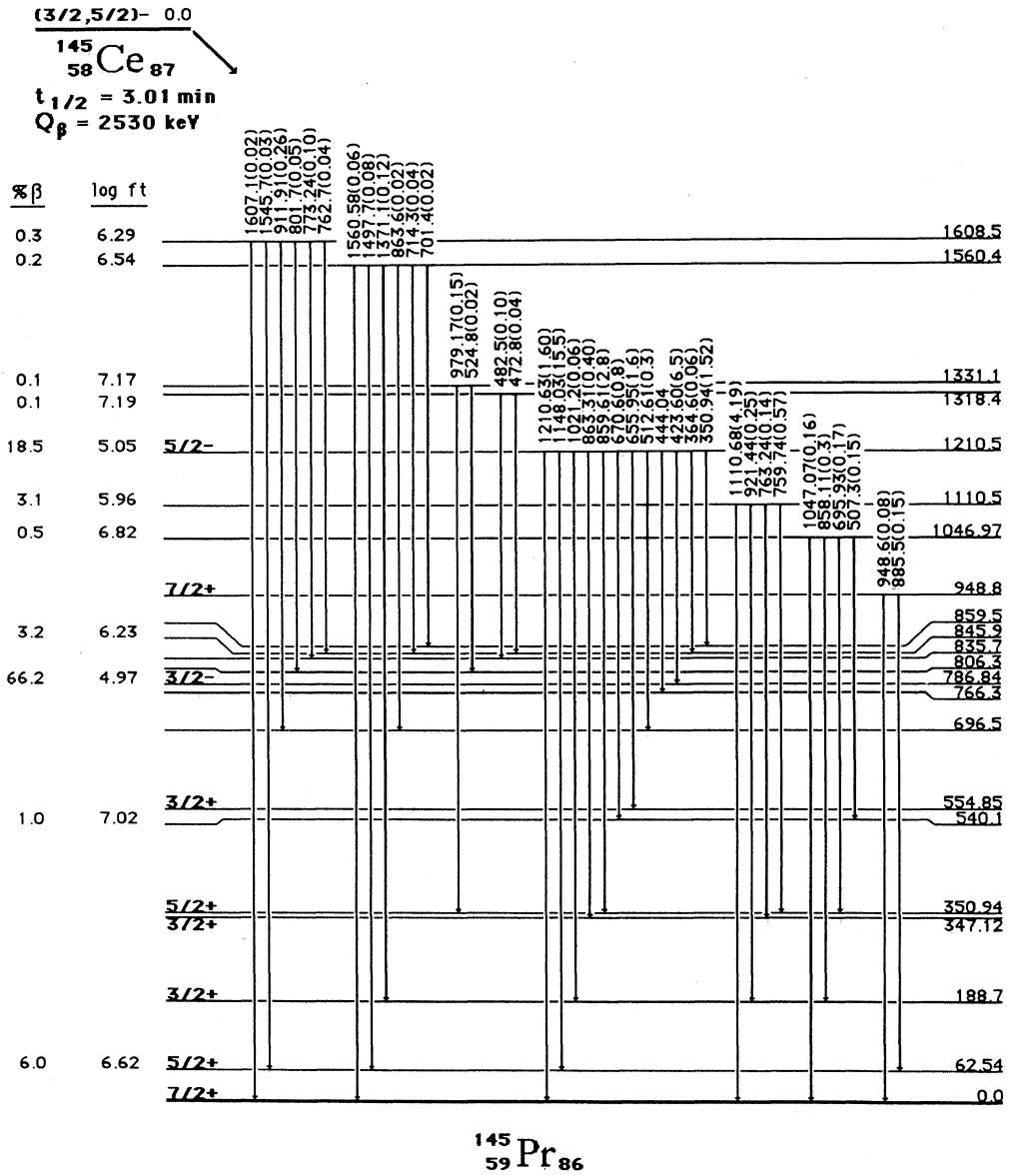

FIG. 3. (*Continued*).

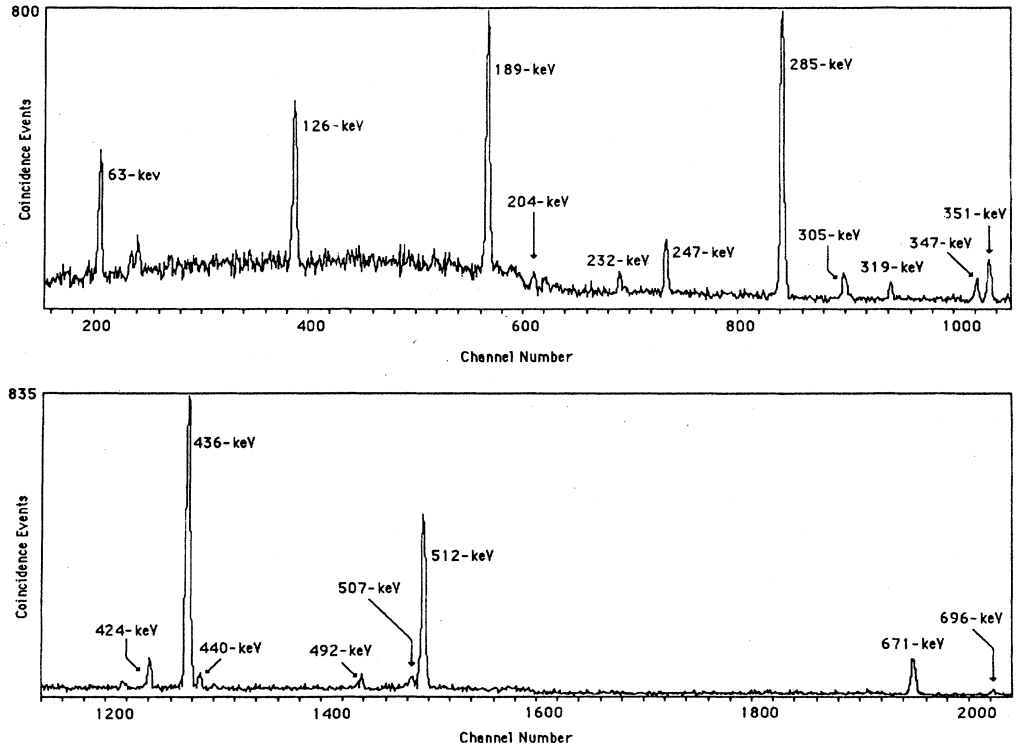

FIG. 4. Spectrum of gamma rays in coincidence with the peak at 351 keV.

tirely by the 351-keV transition between the higher energy levels.

The doublet at 507 keV is suggested by the intensity of the 126- and 189-keV peaks in the spectrum gated on the 507-keV peak. The intensity of the 351-keV peak is only $\frac{2}{3}$ of the combined intensity of the 126- and 189-keV peaks. This intensity imbalance supports the presence of a 507-keV transition that directly populates the 189-keV level.

While the doublet at 773 keV is not distinguished in coincidence spectra, the peak does appear in its own gate, requiring two transitions of that approximate energy. The positions of the individual members of doublets at 656/657, 762/763, and 858/859 keV are distinguished in coincidence spectra.

The absence of an 859-keV transition from the 859-keV level to the ground state cannot be completely established. The 288/351 ratio in the gate on the 859-keV peak is consistent with the singles ratio, but the small size of the 288-keV peak does not exclude up to 0.25 intensity units from depopulating the level at 859 keV.

IV. SPIN AND PARITY ASSIGNMENTS

Eight transitions were assigned l values in the ^{146}Nd$(d,{}^3$He$)^{145}$Pr reaction by van den Berg *et al.*[30] These included transitions to levels at 0(l=4), 60(l=2), 190(l=2), 550(l=4), 760(l=1), 810(l=2), 960(l=4), and 1090(l=2) keV. The l values for the ground and first excited levels and the $M1$ transition between them are consistent with the long established spin and parity assignments of $\frac{7}{2}^+$ and $\frac{5}{2}^+$, respectively. The l=1 transition at 760 keV can be identified with the strongly beta-populated negative-parity level that is at 787 keV which shows no gamma-ray population of the $\frac{7}{2}^+$ ground state. Only a $\frac{3}{2}^-$ assignment is consistent with these data.

The angular anisotropy data for coincidences with the 424-keV gamma ray that populates the 787-keV level may be used for additional spin and parity assignments. Because all of the depopulating transitions have $E1$ multipolarity, they can populate only $\frac{1}{2}^+$, $\frac{3}{2}^+$, and $\frac{5}{2}^+$ levels. Because the levels actually populated by the $\frac{3}{2}^-$ 787-keV level also populate the $\frac{7}{2}^+$ ground state, their spins and parities are limited to $\frac{3}{2}^+$ and $\frac{5}{2}^+$. The anisotropy data show the same ratios at 90° and 180° for the 724- and 436-keV transitions, and a significantly different ratio for the 232- and 439-keV gamma rays. As the 724-keV gamma ray populates a $\frac{5}{2}^+$ level, the 351-keV level populated by the 436-keV transition must also be a $\frac{5}{2}^+$ level. The other levels at 555 and 347 keV populated by the 232- and 439-keV gamma rays, respectively, therefore cannot be $\frac{5}{2}^+$ levels and must be $\frac{3}{2}^+$ levels. Because the 1211-keV level populates both $\frac{3}{2}^+$ levels at 347 and 555 keV as well as the lower-energy $\frac{5}{2}^+$ and $\frac{7}{2}^+$ levels, it must be a $\frac{5}{2}^-$ level.

Two excited l=4 levels were identified by van den Berg *et al.*[30] near 550 and 960 (±20) keV. We have identified the very weakly populated level at 949 keV with the upper l=4 level, but cannot identify either the 540- or 555-keV levels with the lower l=4 level as both of these

levels are populated by the $\frac{3}{2}^-$ level at 787 keV. We do note, however, that the unplaced gamma rays at 517 and 431 keV sum to the energy of the $\frac{7}{2}^+$ level at 948 keV and could indicate that the lower $l=4$ level lies at 517 keV. It would not be surprising if one or more of the unplaced gamma rays at 403, 447, and 645 keV also represent ground-state transitions from missing $\frac{7}{2}^+$, $\frac{9}{2}^+$, and $\frac{11}{2}^+$ levels that should lie in this energy range. These transitions are quite weak and do not appear in any coincidence gates.

The $l=2$ population for the 189-keV level restricts its spin and parity to $\frac{3}{2}^+$ or $\frac{5}{2}^+$. The small strength of the transition in the pickup reaction suggests low proton occupancy and favors the $\frac{3}{2}^+$ assignment. The levels at 806 and 836 keV are the lowest-energy levels that are not populated by the 1211-keV $\frac{5}{2}^-$ level and that do not populate the $\frac{7}{2}^+$ ground state. Either of these levels could be a candidate for the lowest-energy $\frac{1}{2}^+$ level. The absence of significant beta branching to any identified $\frac{7}{2}^+$ levels suggests that the ground-state spin and parity of ^{145}Ce is likely to be $\frac{3}{2}^-$.

V. DISCUSSION

The low-energy levels of the odd-Z Pr nuclides near the closed shell at $N=82$ are shown in Fig. 5. These systematics reveal the two important features of ^{145}Pr not present in the lighter Pr nuclides, the significantly differing ordering of the $\frac{3}{2}^+$ and $\frac{7}{2}^+$ levels in the four-particle nuclide relative to the four-hole nuclide,[40] and the presence of a low-energy $\frac{3}{2}^-$ level. No low-energy, low-spin, negative-parity levels have been observed in either ^{137}Pr or in ^{139}Pr, although both are populated in the beta decay of a $\frac{1}{2}^+$ parent that should readily populate $\frac{1}{2}^-$ and $\frac{3}{2}^-$ levels.[41] These low-energy negative parity levels do fit in the $N=86$ sequence of isotones as shown in Fig. 6, where similar low-spin levels have been identified in both ^{141}Cs and ^{143}La. Similar low-spin negative-parity levels have not been identified in ^{147}Pm or in ^{149}Eu, but have been established[42] in ^{149}Pm as shown in Fig. 7. The low-spin negative-parity levels in the Pm nuclides were not fitted in the IBFM calculations of Scholten and Blasi.[1] The Pm nuclides have been particularly attractive for theoretical study because of the completeness of the identification of the particle-phonon levels built on the $d_{5/2}$ and $g_{7/2}$ levels in both nuclides. Relatively complete sets of negative-parity levels are also identified in both Pm nuclides. They clearly reveal the particle-phonon structure as well as the extraordinary low-energy $\frac{3}{2}^-$ and $\frac{5}{2}^-$ levels that appear to be only present in ^{149}Pm. The multiplets themselves are interesting as the $d_{5/2}$ multiplets in both nuclides are nearly degenerate at the phonon energy as contrasted with the $g_{7/2}$ multiplets which are much more spread out. The negative-parity multiplets show the presence of a depressed j-2 $\frac{7}{2}$ level with an intermediate mixing of the particle-phonon multiplet. That the $\frac{3}{2}^-$ and $\frac{5}{2}^-$ levels in ^{149}Pm represent a separate structure is attested to by the relatively weak $M1/E2$ branches to the $\frac{7}{2}^-$ level as compared to the $E1$ transitions to the positive-parity levels. There appear to be two configurations present with negative-parity. These include low-seniority configurations with the odd particle in the $h_{11/2}$ level where excited levels arise from coupling with the adjacent 2^+ phonon, as well as more complex structures with higher seniority and larger deformation that gives rise to the low-energy $\frac{3}{2}^-$ and $\frac{5}{2}^-$ levels.

It is also interesting to note the near absence of degeneracy of levels above the 2^+ phonon energy in ^{145}Pr. The interaction strength is of sufficient magnitude to bring about considerable mixing among the various configurations with consequent movement of levels into the gap between the 2^+ and 4^+ levels in the ^{144}Ce core. A similar feature is observed in both ^{137}Pr and ^{143}Pr, but not so strongly in ^{139}Pr below the $N=82$ closed shell where a considerable gap exists between the group of levels near the 800-keV energy of the first 2^+ level and the

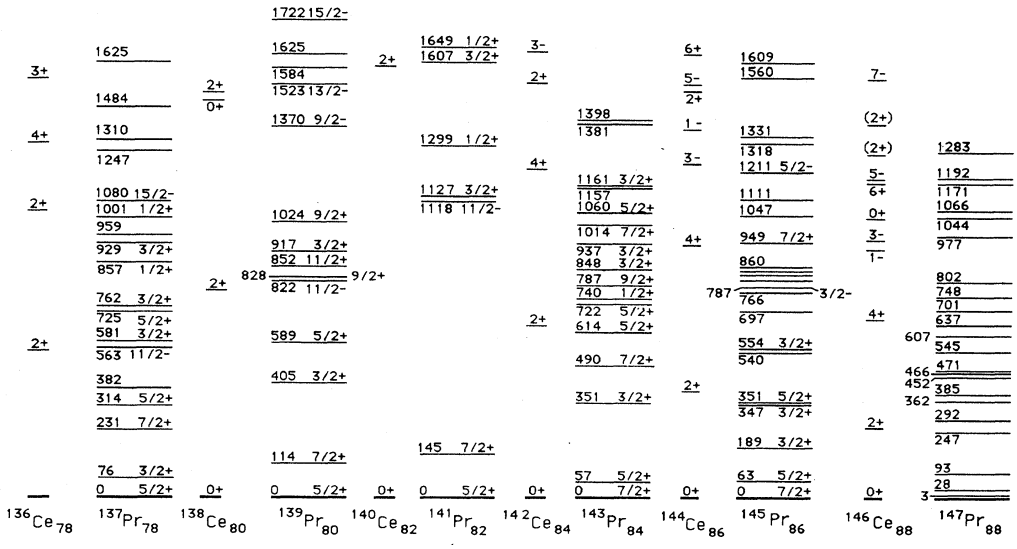

FIG. 5. Positions of the low-energy levels in the odd-mass Pr isotopes.

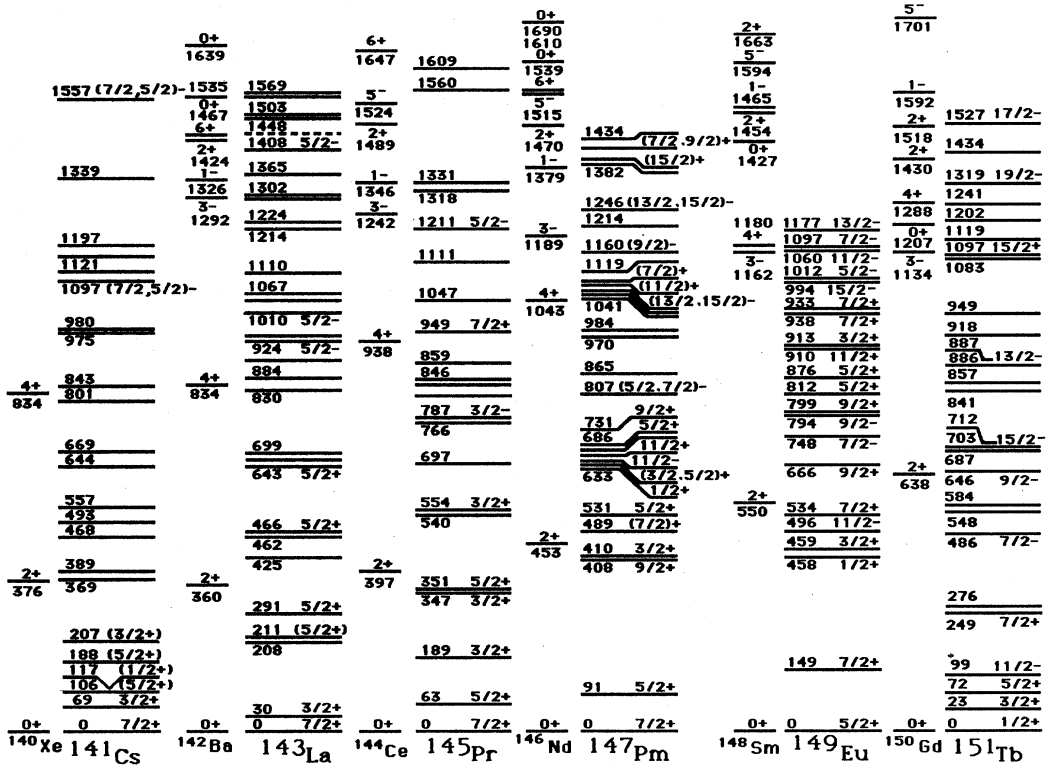

FIG. 6. Positions of the low-energy levels of the $N=86$ isotopes.

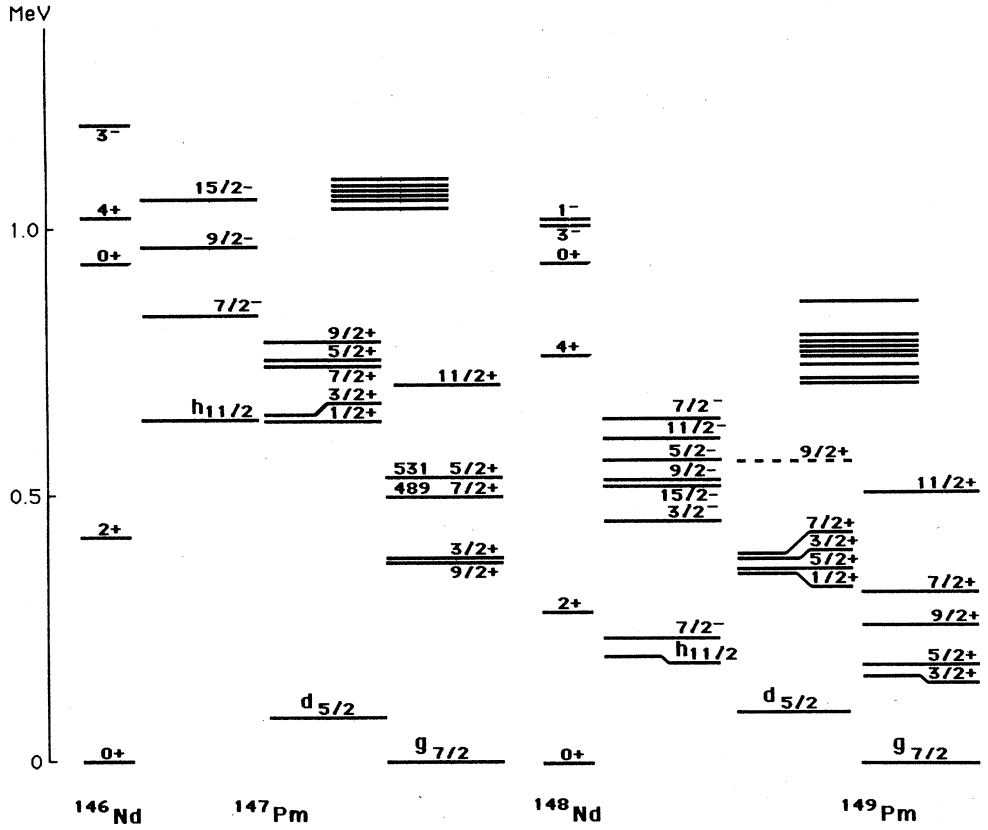

FIG. 7. Low-energy level structures of the odd-Z Pm nuclides ^{147}Pm and ^{149}Pm.

1500-keV energy of higher core excitations.

The positive-parity levels in both ^{143}Pr and ^{145}Pr are reasonably well accounted for by an IBFM calculation.[35] The resulting level scheme is shown in Fig. 8 and the wave functions tabulated in Table IV. The IBFM parameters used are tabulated in Table V. The parameters for the Ce core were established in calculations of the levels of both the even-even Nd nuclides and Ce nuclides. They were compared with earlier results of Snelling and Hamilton.[43] The parameters listed in Table V may be compared with those used by Scholten and Ozzello[2] in their IBFM calculations for the levels of the odd-mass Pm nuclides. For isotonic $N=86$ ^{147}Pm, the Λ_0 is found to be in close agreement with the one they use for the positive-parity levels of the Pm nuclides, while the Γ_0 compares with the one they use for the negative-parity levels of the Pm nuclides and is considerably higher than that for the positive-parity levels. Inasmuch as there are two less protons in Pr than in Pm, the occupancy values of near 50% for $g_{7/2}$ and $d_{5/2}$ levels are in good agreement with the 64 % values that they propose for those orbitals in ^{147}Pm. Both calculations indicate the shift of one pair of protons largely out of the $g_{7/2}$ orbital into the $h_{11/2}$ orbital as compared to the occupancies at the closed shell[4-6] for ^{143}Pr and ^{145}Pm. These calculations are able to describe the inversion of the $\frac{5}{2}^+$ and $\frac{7}{2}^+$ low-energy levels and with the lowered position of the $\frac{3}{2}^+$ level. The level densities are in good agreement for both nuclides in spite

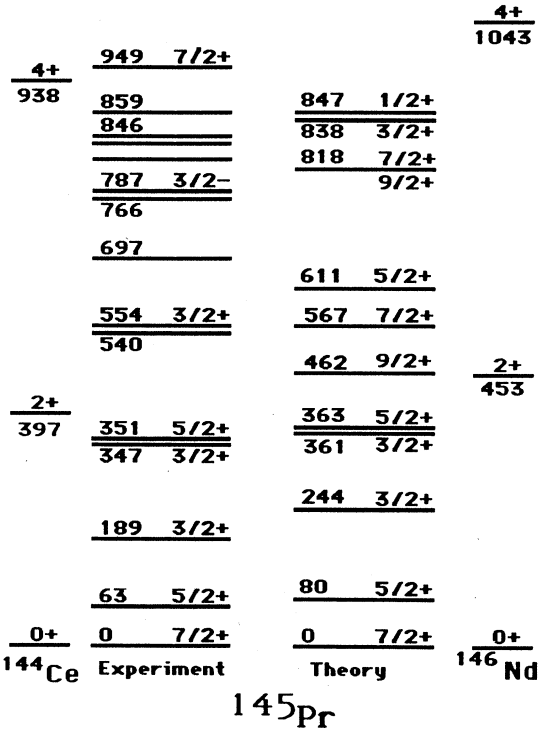

FIG. 8. Comparison of experimental and IBFM calculated levels for ^{145}Pr.

TABLE IV. Wave functions for the low-energy positive-parity states in the $Z=59$ nuclides ^{143}Pr and ^{145}Pr.

$2J^a$	$2j$ (See b)	N	I	Amplitude ($\times 10^3$) 143	145	$2J^a$	$2j$ (See b)	N	I	Amplitude ($\times 10^3$) 143	145
7(1)	7	0	0	644	510	5(2)	7	1	2	469	233
		1	2	185	221			2	2	88	127
		2	0	113	159			2	4	13	11
		2	4					3	2	63	70
		3	0					3	3		15
		3	2	18	40			4	2		20
		4	0		11		5	0	0	107	167
	3	1	2	21	25			1	2	103	40
		2	2					2	0	25	70
		3	2					2	2	30	46
5(1)	7	1	2	64	134			2	4	60	110
		2	2		28			3	0		
		3	2		35			3	2	13	12
		3	3					3	4		16
		4	2					4	0		
		4	2′					4	2		
		5	2					4	4		18
	5	0	0	666	437			5	4		
		1	2	97	130		3	1	2		
		2	0	113	132			2	2		
		2	2					3	2		
		2	4			7(2)	7	0	0	23	11
		3	0					1	2	117	63
		3	2		26			2	0	19	23
	3	1	2	21	28			2	2		
3(1)	7	1	2	31	19			2	4	287	263
		2	2					3	0		12

TABLE IV. (*Continued*).

$2J^a$	$2j$ (See b)	N	I	Amplitude ($\times 10^3$) 143	145		$2J^a$	$2j$ (See b)	N	I	Amplitude ($\times 10^3$) 143	145	
		3	2						3	2	13	13	
		3	3						3	3		12	
		4	2						3	4		64	
	5	1	2	714	570				4	0			
		2	2	18	39				4	4	19	42	
		2	4	21	33				4	5			
		3	2	86	140				5	4			
		3	3					5	1	2	244	176	
		4	2						2	2	103	127	
		4	2′						2	4	62	54	64
		4	4						3	2	30	43	28
		5	2						3	4		17	45
	3	0	0	53	54				3	6			
		1	2	29	38				4	2		17	17
		2	0	13	22				4	4			17
		2	2		14			3	2	4	12	13	
		3	2		10		5(3)	7	1	2	189	175	
3(2)	7	1	2	503	403				2	2	34		
		2	2	261	315				2	4	134	179	
		3	2	61	97				3	2	13	23	
		3	3		13				3	3			
		4	2	15	41				3	4	15	59	
	5	1	2						4	4		27	
		2	2						4	4′			
		2	4						4	5			
		3	2						5	4			
		3	3					5	0	0			
		3	4						1	2	143	90	
		4	2						2	0			
		4	2′						2	2	76	69	
		4	4						2	4	257	160	
		5	2						3	0			
	3	0	0	100	63	36			3	2	18	23	
		1	2						3	4	14	21	
		2	0	36	40	35			4	4	16	23	
		2	2					3	1	2	37	45	
		3	0			11			2	2	24	33	
		3	2						3	2		17	

[a]This column gives twice the J value of the n_{th} J (n in parentheses) level, i.e., we label the first $\frac{7}{2}^+$ level, $\frac{7}{2}^+$ (1) as 7(1).

[b]The second column gives twice the orbital value where $3 \equiv d_{3/2}$, $5 \equiv d_{5/2}$, and $7 \equiv g_{7/2}$. The third column N gives the number of bosons coupled to 2^+. The fourth column I gives the total angular momentum of the bosons coupled to 2^+. The seventh row of the table thus reveals that the amplitude of the component of the first $\frac{7}{2}^+$ level that involves a $g_{7/2}$ proton coupled to three 2^+ bosons that are themselves coupled to angular momentum 2 is 0.018, while the ninth row indicates the amplitude of component of the first $\frac{7}{2}^+$ level that involves a $d_{3/2}$ proton coupled to a single 2^+ boson is 0.021.

of the lack of precise spin assignments. As 91% of the beta decay of the ^{145}Ce populates the two negative-parity levels, it is not surprising that the $\frac{7}{2}^+$ and $\frac{9}{2}^+$ levels indicated in the calculation and identified in the transfer reaction studies are not found in this study.

There is some qualitative and quantitative support for the rather low single-particle occupancy values indicated in Table IV for the lowest $\frac{7}{2}^+$ (0.64 and 0.51) and $\frac{5}{2}^+$ (0.67 and 0.44) levels in ^{143}Pr and ^{145}Pr, respectively. The qualitative support comes from examination of the (d,^{3}He) spectra for pickup of a proton from Nd into Pr levels exhibited by Van den Berg *et al.*[30] In those spectra, only the five single-particle levels are populated in the semimagic ^{141}Pr with the $d_{5/2}$ ground state and $g_{7/2}$ first excited state showing very large peaks. For the same reaction populating ^{145}Pr and ^{149}Pr, the spectra are seen to be much more complex showing reduced height relative to the other peaks indicating that the single-particle strength spreads steadily with increasing neutron number. Quantitative support comes from the C^2S values shown in Figs. 1 and 2 for the (^{3}He,d) reactions populating ^{143,145}Pm. These spectroscopic values are a product of single-particle character and vacancy. The values show a significant increase in C^2S for the $g_{7/2}$ orbital

TABLE V. Parameters used for the odd-mass IBFM calculations for ^{143}Pr and ^{145}Pr.

Isotope	Γ_0 MeV	Λ_0 MeV	A_0 MeV	ν^2 $g_{7/2}$	$d_{5/2}$	$d_{3/2}$	e_{gd}[a] MeV	e_{dd}[b] MeV
^{143}Pr	1.17	0.60	0	0.746	0.380	0.024	0.094	1.80
^{145}Pr	1.17	0.60	0	0.748	0.380	0.024	0.098	1.78

[a]This column gives the energy difference adopted between the $g_{7/2}$ and $d_{5/2}$ orbitals.
[b]This column gives the energy difference adopted between the $d_{3/2}$ and $d_{5/2}$ orbitals.

with the addition of two neutrons indicating that the vacancy has been substantially increased while showing considerably lower C^2S values for the other orbitals indicating reduced vacancy for the other single-particle levels. That is, the addition of even one pair of neutrons results in a considerable movement of proton occupancy from the $g_{7/2}$ orbital into the other orbital. Moreover, just the fact that the positions of the $d_{5/2}$ and $g_{7/2}$ invert with the addition of two neutrons to closed shell ^{141}Pr indicates a considerable increase in the complexity of the wave function for both levels.

These calculations may be compared with those of Aryaeinejad and McHarris[41] for ^{139}Pr which has $N=80$. Both calculations obtain second $\frac{5}{2}^+$ and $\frac{3}{2}^+$ levels that are depressed below the energy of the 2^+ level in the adjacent even-even nuclide, while the other particle plus core levels are nearly degenerate with the 2^+ core energy. Aryaeinejad and McHarris[41] used a triaxial model with gamma near 34° in their calculations and were also interested in fitting levels up to considerably higher spin.

The levels of ^{137}Pr were interpreted by Klewe-Nebenius *et al.*[40] to indicate strong coupling and prolate deformation with a $\beta=+0.11$. That interpretation would appear to be flawed by the absence of any evidence for the $\frac{1}{2}^-$ [550] and $\frac{3}{2}^-$ [541] levels. The presence of a low-energy $\frac{11}{2}^-$ level that either arises from oblate deformation or from the single-particle $h_{11/2}$ orbital does not support strong coupling. Moreover, the $\frac{15}{2}^-$, $\frac{19}{2}^-$, and $\frac{23}{2}^-$ levels lie at almost exactly the energies of the core ^{136}Ce 2^+, 4^+, and 6^+ levels, respectively. Although the introduction of triaxiality for the interpretation of the levels of ^{139}Pr may be of some value in the interpretation of the positive-parity levels, it has the effect of pushing the $\frac{19}{2}^-$ and $\frac{23}{2}^-$ levels far above their observed positions. Again, as in ^{137}Pr, the $\frac{19}{2}^-$ level in ^{139}Pr lies in close proximity to the 4^+ level of the ^{138}Ce core.

The absence of identification of the $h_{11/2}$ level in ^{145}Pr is a considerable barrier to an understanding of the structure of the negative-parity levels. It is possible to interpret the $\frac{3}{2}^-$ level at 787 keV as the $\frac{3}{2}^-$ [541] level, but there is no evidence for a $\frac{5}{2}^-$ level at an energy that would indicate a prolate rotational structure. The $\frac{3}{2}^-$ and $\frac{5}{2}^-$ levels that are observed appear to be separate from the other levels in a manner comparable to the $\frac{3}{2}^-$ and $\frac{5}{2}^-$ levels in ^{149}Pm. That is, they are not populated by any transitions from other levels and they are strongly populated in beta decay. There must surely be numerous negative-parity levels above 1200 keV arising from coupling of the $g_{7/2}$ and $d_{5/2}$ single-particle levels with the well established 3^- and 1^- levels in the core ^{144}Ce. Yet, there are no other levels that are strongly populated in beta decay and if any of the higher-energy levels identified in ^{145}Pr are negative parity, they auspiciously avoid gamma-ray population to the two strongly beta-populated negative-parity levels. This limited range of the beta population could be interpreted as indicating that the ground state of ^{145}Ce is more strongly deformed and that beta decay strongly populates the two-energy levels in ^{145}Pr that are also comparably deformed. In contrast, when the odd proton is in either of the positive-parity $g_{7/2}$ or $d_{5/2}$ levels, the nucleus shows structures that do not appear to require unusual deformation to account for the observed levels.

Thus, we conclude by noting that the positive-parity levels appear to be able to be described by two rather different calculational procedures, while the low-energy negative-parity level at 787 keV has thus far defied description. Its presence may be taken as an indication of considerably enhanced deformation relative to the positive-parity levels and as an indication of the importance of high angular-momentum levels in inducing deformation through the strong *n-p* interaction. As this level does have negative parity, it could also indicate that this enhanced deformation originates with the reflection asymmetric structures identified elsewhere in this mass region, particularly in adjacent ^{146}Ce.

ACKNOWLEDGMENTS

The authors appreciate the assistance of Dr. R. L. Gill and Dr. A. Piotrowski and the TRISTAN technical staff during the performance of these experiments and the subsequent reduction of the data as well as the hospitality of Dr. R. F. Casten and the entire Neutron Nuclear Physics Group at Brookhaven National Laboratory. This work was supported by the Office of High Energy and Nuclear Physics of the U.S. Department of Energy under Contracts DE-FG05-88ER40418 with the University of Maryland, and W-7405-Eng-48 at the Lawrence Livermore National Laboratory, and through Brookhaven National Laboratory under Contract DE-AC02-76CH00016.

*Present address: Department of Chemistry, University of Kentucky, Lexington, KY 40506.
†Present address: Building 88, Lawrence Berkeley Laboratory, Berkeley, CA 94720.
‡Present address: Environmental Protection Agency, Las Vegas, NV 89193.
§Present address: Center for Analytical Chemistry, National Bureau of Standards, Gaithersburg, MD 20899.
**Present address: National Superconducting Cyclotron Laboratory, Michigan State University, East Lansing, MI.

[1]O. Scholten and N. Blasi, Nucl. Phys. **A380**, 509 (1982).
[2]O. Scholten and T. Ozzello, Nucl. Phys. **A424**, 22 (1984).
[3]R. F. Casten, W. Frank, and P. von Brentano, Nucl. Phys. **A444**, 133 (1985).
[4]B. H. Wildenthal, E. Newman, and R. L. Auble, Phys. Rev. C **3**, 1199 (1973).
[5]M. Waroquier and K. Heyde, Nucl. Phys. **A144**, 481 (1970).
[6]N. Freed and W. Miles, Nucl. Phys. **A158**, 230 (1970).
[7]Y. Nagai, J. Styczen, M. Piiparinen, P. Kleinheinz, D. Bazzacco, P. v. Brentano, K. O. Zell, and J. Blomqvist, Phys. Rev. Lett. **47**, 1259 (1981).
[8]K. Heyde, M. Waroquier, H. Vincx, and P. J. Brussard, Nucl. Phys. **A234**, 216 (1974).
[9]W. B. Walters, C. Chung, D. S. Brenner, A. Aprahamian, R. L. Gill, R. Chrien, M. Shmid, A. Wolf, and L.-J. Yuan, Phys. Lett. **125B**, 351 (1983).
[10]O. Straume, G. Lovhoiden, and D. G. Burke, Z. Phys. A **295**, 259 (1980).
[11]S. H. Faller, C. A. Stone, J. D. Robertson, C. Chung, N. K. Aras, W. B. Walters, R. L. Gill, and A. Piotrowski, Phys. Rev. C **34**, 654 (1986).
[12]W. J. Baldridge, Phys. Rev. C **18**, 530 (1978).
[13]M. Samri, G. J. Costa, G. Klotz, D. Magnac, R. Seltz, and J. P. Zirnheld, Z. Phys. A **321**, 255 (1985).
[14]I. L. Lee, W. J. Jordan, J. V. Maher, R. Kamermans, J. W. Smits, and R. H. Siemssen, Nucl. Phys. **A371**, 111 (1981).
[15]S. A. Ahmad, W. Klempt, C. Ekstrom, R. Neugart, and K. Wendt, Z. Phys. A **321**, 35 (1985).
[16]D. A. Eastham, J. G. England, D. E. Evans, M. J. Fawcett, I. S. Grant, J. A. R. Griffith, G. W. A. Newton, and P. M. Walker, J. Phys. G **10**, L271 (1984).
[17]A. Wolf, A. Berant, D. D. Warner, R. L. Gill, M. Shmid, R. E. Chrien, G. Peaslee, H. Yamamoto, J. C. Hill, F. K. Wohn, C. Chung, and W. B. Walters, Phys. Lett. **123B**, 165 (1983).
[18]A. Wolf, D. D. Warner, and N. Benczer-Koller, Phys. Lett. **158B**, 7 (1985).
[19]A. Wolf and R. F. Casten, Phys. Rev. C **36**, 851 (1987).
[20]G. A. Leander, W. Nazarewicz, P. Olanders, I. Ragnarsson, and J. Dudek, Phys. Lett. **152B**, 284 (1985).
[21]J. D. Robertson, S. H. Faller, W. B. Walters, R. L. Gill, H. Mach, A. Piotrowski, E. F. Zganjar, H. Dejbakhsh, and R. F. Petry, Phys. Rev. C **34**, 1012 (1986).
[22]W. R. Phillips, I. Ahmad, H. Emling, R. Holzmann, R. V. F. Janssens, T.-L. Khoo, and M. W. Drigert, Phys. Rev. Lett. **57**, 3257 (1986).
[23]H. Iimura, T. Seo, and S. Yamada, J. Phys. Soc. Jpn. **55**, 1108 (1986).
[24]A. Ohyoshi, E. Ohyoshi, T. Tamai, and M. Shinagawa, J. Inorg. Nucl. Chem. **34**, 3293 (1972).
[25]H. Yamamoto, Y. Ikeda, K. Kawade, T. Katoh, and T. Nagahara, J. Inorg. Nucl. Chem. **42**, 1539 (1980).
[26]H. W. Taylor and B. Singh, J. Phys. G **5**, 1445 (1979).
[27]B. Pfeiffer, F. Schussler, J. Blachot, S. J. Feenstra, J. van Klinken, H. Lawin, E. Monnand, G. Sadler, H. Wollnik, and K. D. Wunsch, Z. Phys. A **287**, 191 (1978).
[28]A. Saha, R. H. Siemssen, J. W. Smits, and J. van Popta, Kernfysisch Organization for the Advancement of Pure Research Annual Report 14, 1977.
[29]A. Saha, H. T. Fortune, M. N. Harakeh, J. van Popta, R. H. Siemssen, and S. Y. van der Werf, Kernfysisch Organization for the Advancement of Pure Research Annual Report 7, 1978.
[30]A. M. Van den Berg, M. N. Harakeh, Y. Iwasaki, R. H. Siemssen, and S. Y. van der Werf, Kernfysisch Organization for the Advancement of Pure Research Annual Report 25, 1980.
[31]V. A. Bondarenko, P. T. Prokof'ev, W. Enghardt, H. Prade, F. Stary, L. Koibler, and H.-J. Keller, Bull. Acad. Sci. USSR, Phys. Ser. **50**, 24 (1986).
[32]M. Kortelahti, M. Piiparinen, A. Pakkanen, T. Komppa, R. Komu, S. Brant, Lj. Udovicic, and V. Paar, Nucl. Phys. **A342**, 421 (1980).
[33]S. H. Faller, J. D. Robertson, E. M. Baum, C. Chung, C. A. Stone, and W. B. Walters, Phys. Rev. C **38**, 307 (1988).
[34]S. H. Faller, P. F. Mantica, Jr., J. D. Robertson, E. M. Baum, C. A. Stone, and W. B. Walters, Phys. Rev. C **38**, 905 (1988).
[35]D. F. Kusnezov, D. R. Nethaway, and R. A. Meyer, University of California Radiation Laboratory Report UCRL-96477, 1988 (unpublished).
[36]R. L. Gill and A. Piotrowski, Nucl. Instrum. Methods A **234**, 213 (1985).
[37]W. B. Walters, Hyperfine Interact. **22**, 317 (1985).
[38]A. Piotrowski, R. L. Gill, and D. C. McDonald, Nucl. Instrum. Methods **224**, 1 (1984).
[39]F. Rosel, H. M. Fries, K. Alder, and H. C. Pauli, At. Data Nucl. Data Tables **21**, 293 (1978).
[40]H. Klewe-Nebenius, D. Habs, K. Wisshak, H. Faust, G. Nowicki, S. Goring, H. Revel, G. Schatz, and M. Schwall, Nucl. Phys. **A240**, 137 (1975).
[41]R. Aryaeinejad and W. C. McHarris, Phys. Rev. C **37**, 1855 (1988).
[42]E. W. Schneider, M. D. Glascock, W. B. Walters, and R. A. Meyer, Z. Phys. A **291**, 77 (1979).
[43]D. M. Snelling and W. D. Hamilton, J. Phys. G **9**, 111 (1983).